Electronic Supplementary Material (ESI) for Dalton Transactions.

Supporting Information to

Ferrate(II) complexes with redox-active formazanate ligands

Francesca Milocco, Serhiy Demeshko, Franc Meyer and Edwin Otten*

Contents

X-ray crystallography

Single crystals of compounds **3**, **4** and **5** were mounted on top of a cryoloop and transferred into the cold nitrogen stream (100 K) of a Bruker-AXS D8 Venture diffractometer. Data collection and reduction was done using the Bruker software suite APEX3.[1] The final unit cell was obtained from the xyz centroids of 9884 (**3**), 9426 (**4**) or 9035 (**5**) reflections after integration. A multiscan absorption correction was applied, based on the intensities of symmetry-related reflections measured at different angular settings (*SADABS*). The structures were solved by direct methods using *SHELXS*,[2] and refinement of the structure was performed using *SHLELXL*.[3] For compound **3**, refinement was frustrated by a disorder problem: from the solution it was clear that the tetrabutyl ammonium cation was disordered over two positions. To account for this disorder, a two-site occupancy model was used for which the s.o.f. was refined to 0.58 for the major fraction. Some atoms in the disordered part refined to non-positive definite displacement parameters when allowed to refine anisotropically, and ultimately RIGU instructions were applied to all atoms in the disordered part.

For all structures, the hydrogen atoms were generated by geometrical considerations, constrained to idealised geometries and allowed to ride on their carrier atoms with an isotropic displacement parameter related to the equivalent displacement parameter of their carrier atoms. Crystal data and details on data collection and refinement are presented in Table S1.

Table S1. Crystallographic data for compounds **3**, **4** and **5**.

	3	**4**	**5**
chem formula	$C_{36}H_{53}Br_2Fe\ N_5$	$C_{36}H_{53}Cl_2Fe\ N_5$	$C_{68}H_{77}Br_2FeN_8O$
M_r	771.50	682.60	1270.12
cryst syst	orthorhombic	orthorhombic	triclinic
color, habit	red, needle	red, needle	green, platelet
size (mm)	0.40 x 0.12 x 0.03	0.64 x 0.10 x 0.07	0.22 x 0.20 x 0.03
space group	P 21 21 21	P 21 21 21	P -1
a (Å)	9.4704(3)	9.1098(5)	10.1421(7)
b (Å)	16.8186(5)	16.4746(8)	11.1790(8)
c (Å)	22.8415(7)	23.8401(13)	28.764(2)
α (°)	90	90	87.411(3)
β (°)	90	90	86.537(3)
γ (°)	90	90	77.464(3)
V (Å^3)	3638.17(19)	3577.9(3)	3175.9(4)
Z	4	4	2
ρ_{calc}, g.cm^{-3}	1.409	1.267	1.328
Radiation [Å]	Mo K_α 0.71073	Mo K_α 0.71073	Mo K_α 0.71073
μ(Mo K_α), mm^{-1}	2.643	0.603	0.928
F(000)	1600	1456	1332
Temp (K)	100(2)	100(2)	100(2)
θ range (°)	2.94 – 27.14	3.01 – 27.18	2.88 – 25.68
data collected (h,k,l)	-12:12; -21:21; -29:29	-11:11; -19:21; -30:30	-12:12; -13:13; -35:35
no. of rflns collected	63248	52566	86747
no. of indpndt collected	8038	7904	12053

Observed reflns $F_o \geq 2.0\ \sigma(F_o)$	7566	7410	10625
R(F) (%)	1.65	2.33	4.03
wR(F^2) (%)	3.81	5.56	9.26
GooF	1.024	1.048	1.121
weighting a,b	0.0152, 0	0.0254, 0.7065	0.0125, 7.4846
params refined	560	402	780
min, max resid dens	-0.302, 0.256	-0.276, 0.183	-0.809, 0.820

Table S2. Pertinent interatomic distances and bond angles in compounds **3**, **4** and **5**.

	3 (X = Br)	**4** (X = Cl)	**5**
Fe(1) – N(1)	1.9785(17)	1.9830(17)	1.970(2)
Fe(1) – N(4)	1.9765(17)	1.9817(17)	1.978(2)
Fe(1) – X(1)	2.4176(4)	2.2774(6)	
Fe(1) – X(2)	2.4182(3)	2.2898(6)	
N(1) – N(2)	1.317(2)	1.317(2)	1.290(3)
N(3) – N(4)	1.313(2)	1.317(2)	1.282(3)
N(2) – C(7)	1.346(2)	1.347(2)	1.353(3)
N(3) – C(7)	1.346(3)	1.348(2)	1.357(3)
N(1) – Fe(1) – N (4)	91.38(7)	91.49(7)	83.96(9)
X(1) – Fe(1) – X(2)	108.304(13)	107.59(2)	
(N – Fe – N)/ (X – Fe – X)	86.72	88.16	

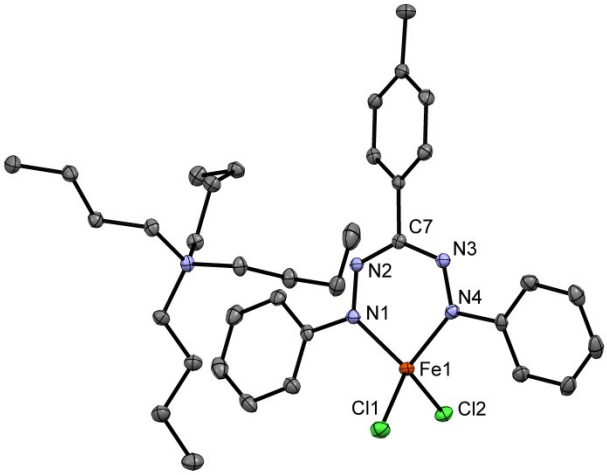

Figure S1. Molecular structure of compound **4** showing 50% probability ellipsoids. Hydrogen atoms, and one of the disorder components of the Bu_4N moiety are omitted for clarity.

Mössbauer spectroscopy

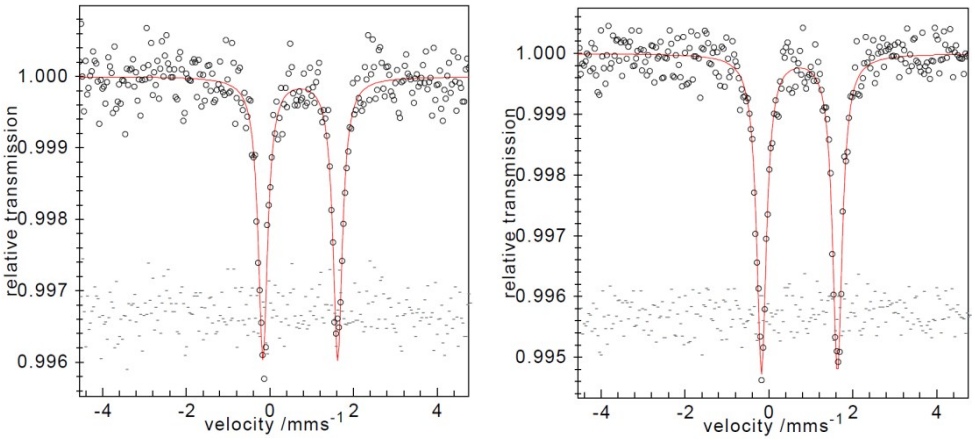

Figure S2. Zero-field Mössbauer spectra of solid **3** at 80 K (left; fit parameters are δ = 0.73 mm·s^{-1} and ΔE_Q = 1.79 mm·s^{-1}) and at 7 K (right; fit parameters are δ = 0.73 mm·s^{-1} and ΔE_Q = 1.81 mm·s^{-1}).

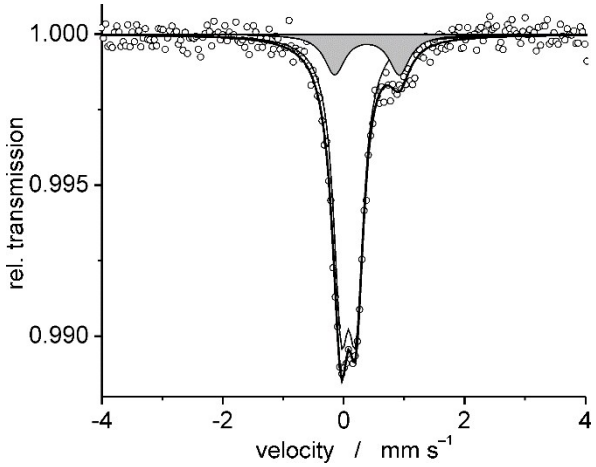

Figure S3. Zero-field Mössbauer spectrum of solid **5** at 80 K. Data is fit with two contributions: parameters for the major fraction (82%) are δ = 0.08 mm·s^{-1} and ΔE_Q = 0.25 mm·s^{-1}; parameters for the minor fraction (18%) are δ = 0.39 mm·s^{-1} and ΔE_Q = 1.07 mm·s^{-1}.

NMR spectral data

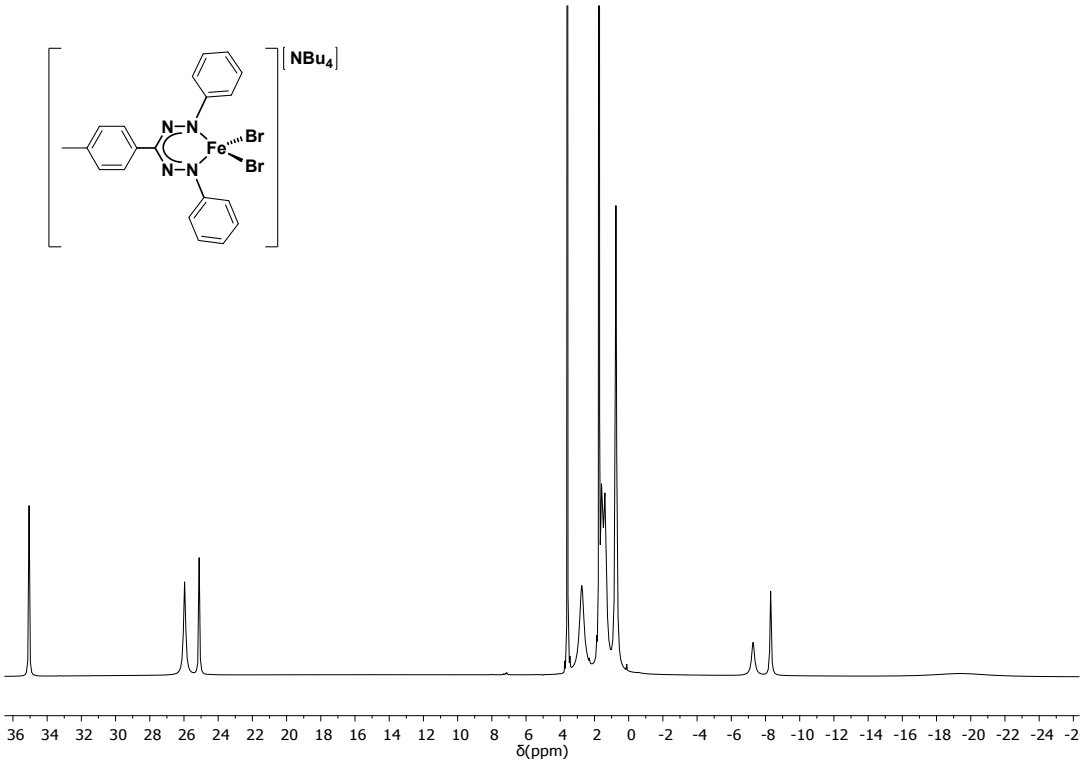

Figure S4a. ^{1}H NMR spectrum of **3** (THF-d_8, 500 MHZ, 25 °C).

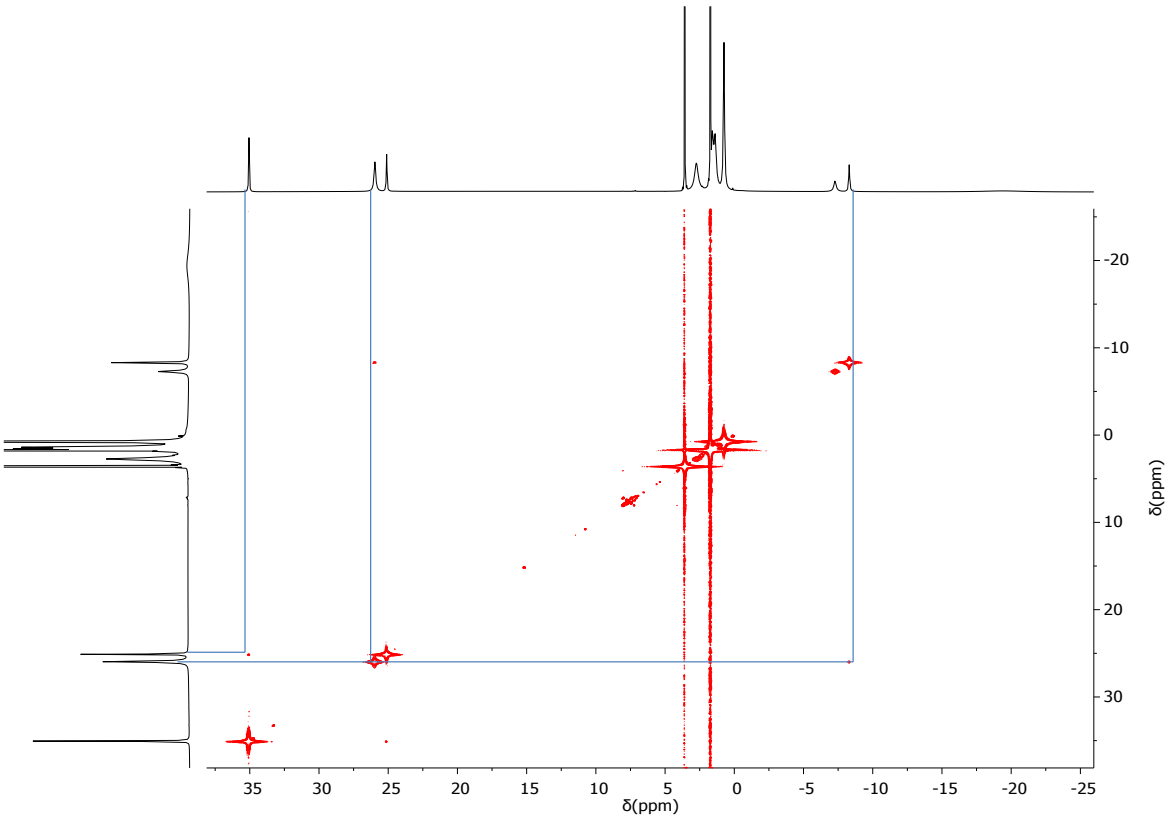

Figure S4b. ^{1}H-^{1}H COSY spectrum of **3** (THF-d_8, 500 MHZ, 25 °C).

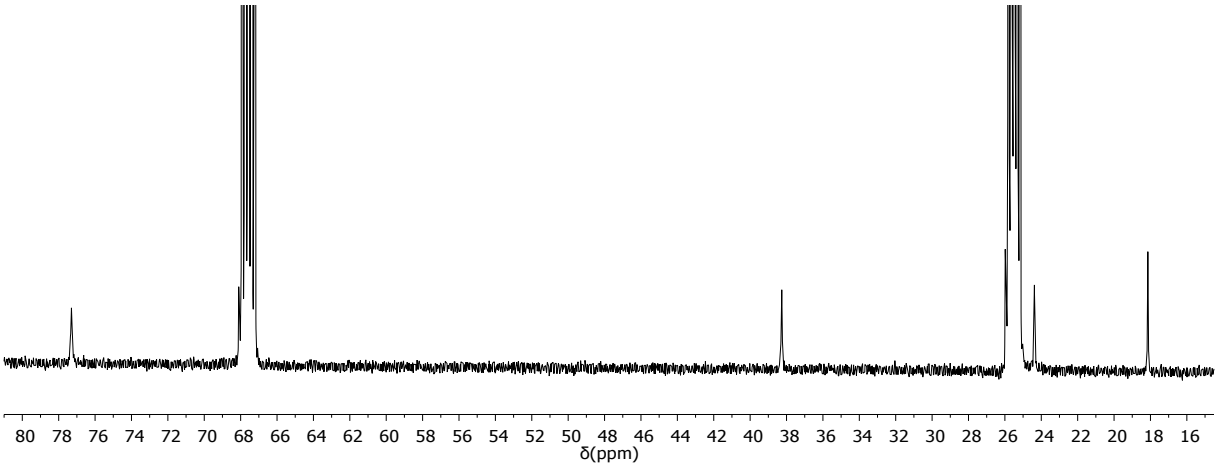

Figure S4c. ^{13}C NMR spectrum of **3** (THF-d_8, 500 MHZ, 25 °C).

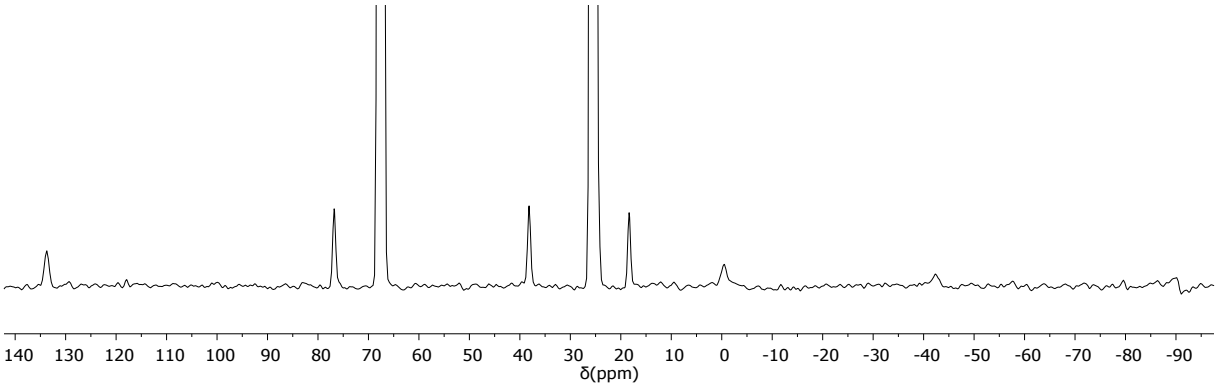

Figure S4d. ^{13}C NMR spectrum of **3** (THF-d_8, 500 MHZ, 25 °C, relaxation delay = 0.5 s).

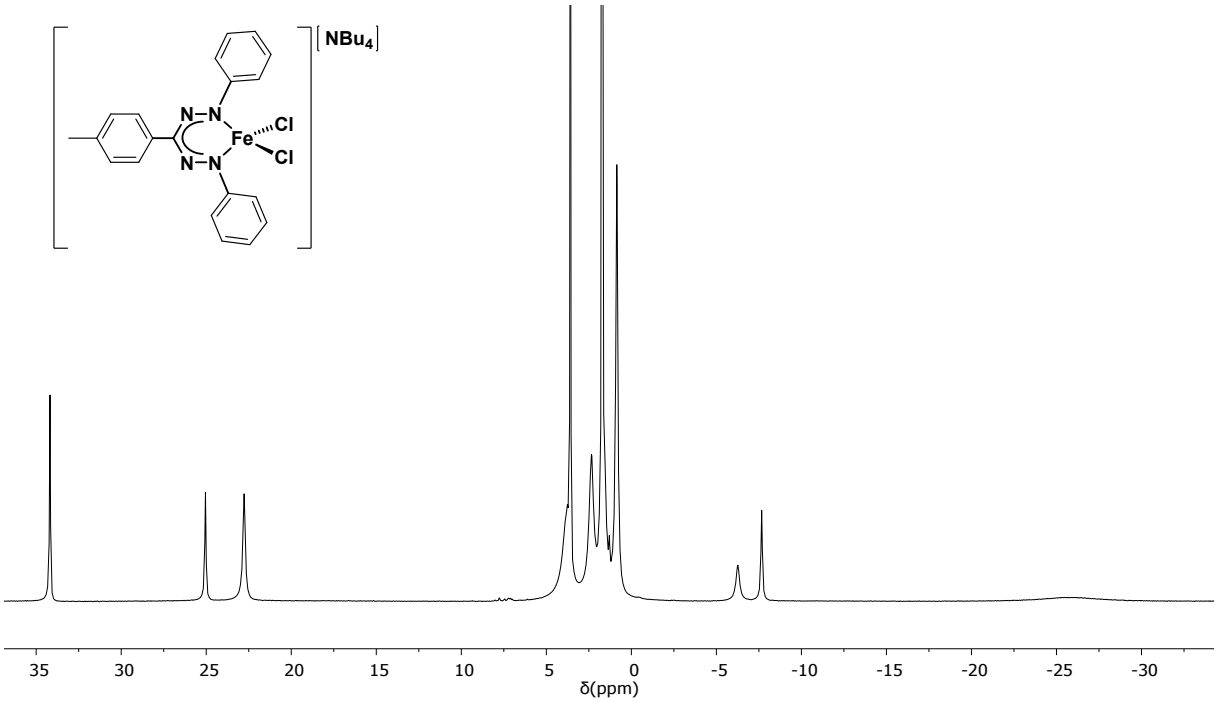

Figure S5a. ^{1}H NMR spectrum of **4** (THF-d_8, 400 MHZ, 25 °C).

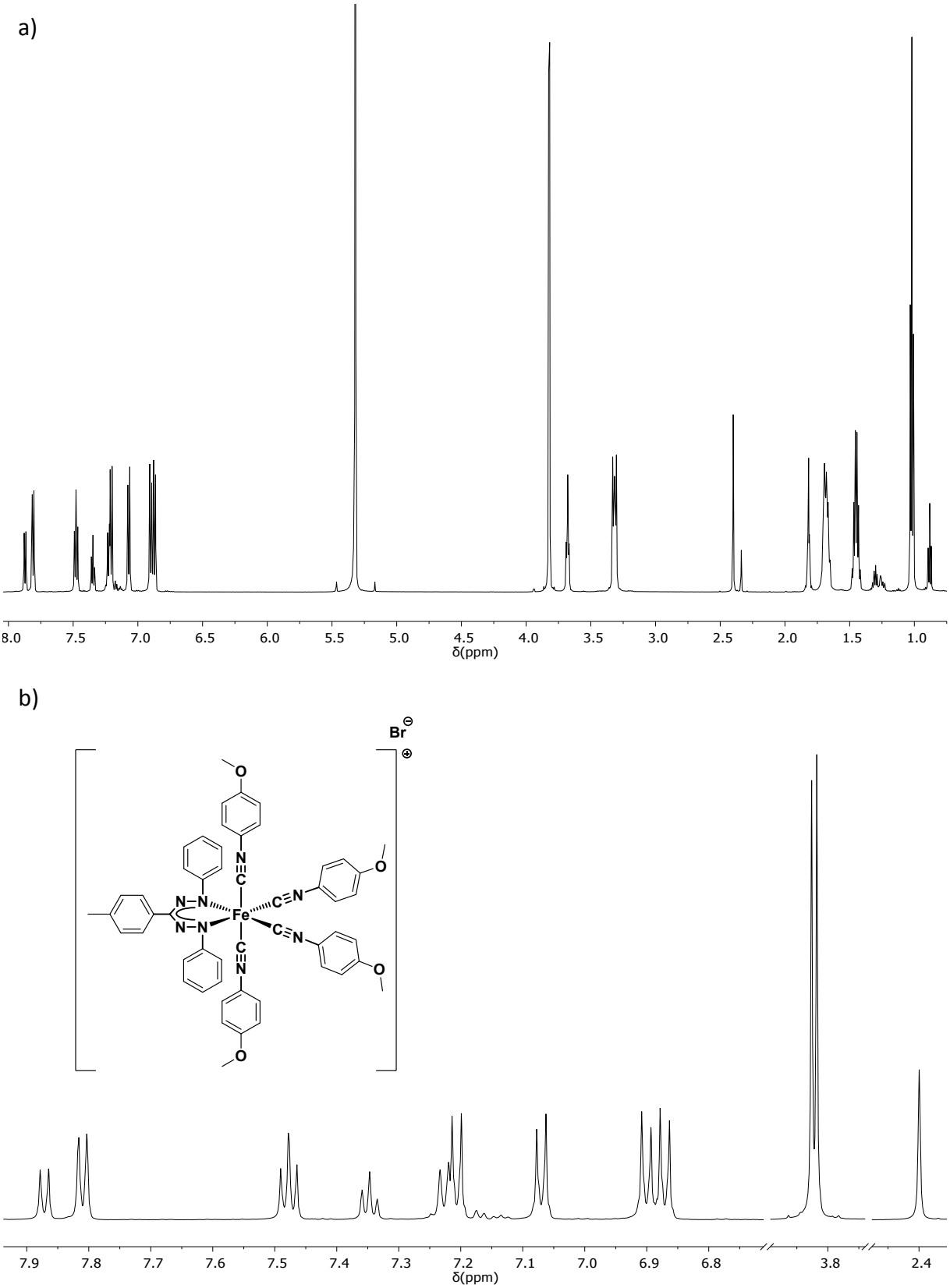

Figure S6a. ^{1}H NMR spectrum of **5** + NBu_4Br (CD_2Cl_2, 600 MHZ, 25 °C): a) full spectrum, b) selected peaks of **5**.

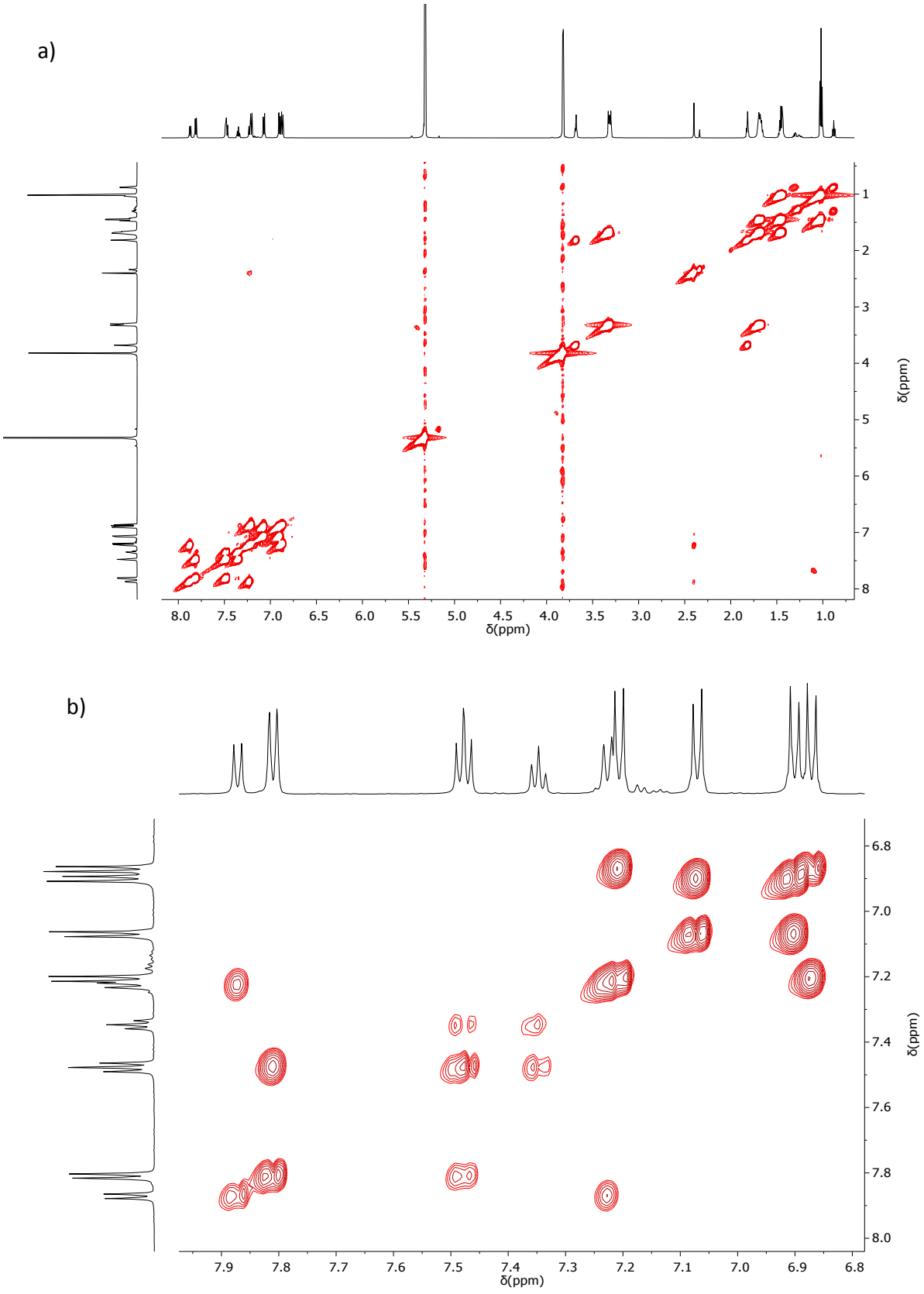

Figure S6b. ^{1}H-^{1}H COSY spectrum of **5** + NBu_4Br (CD_2Cl_2, 600 MHZ, 25 °C): a) full spectrum, b) aromatic region.

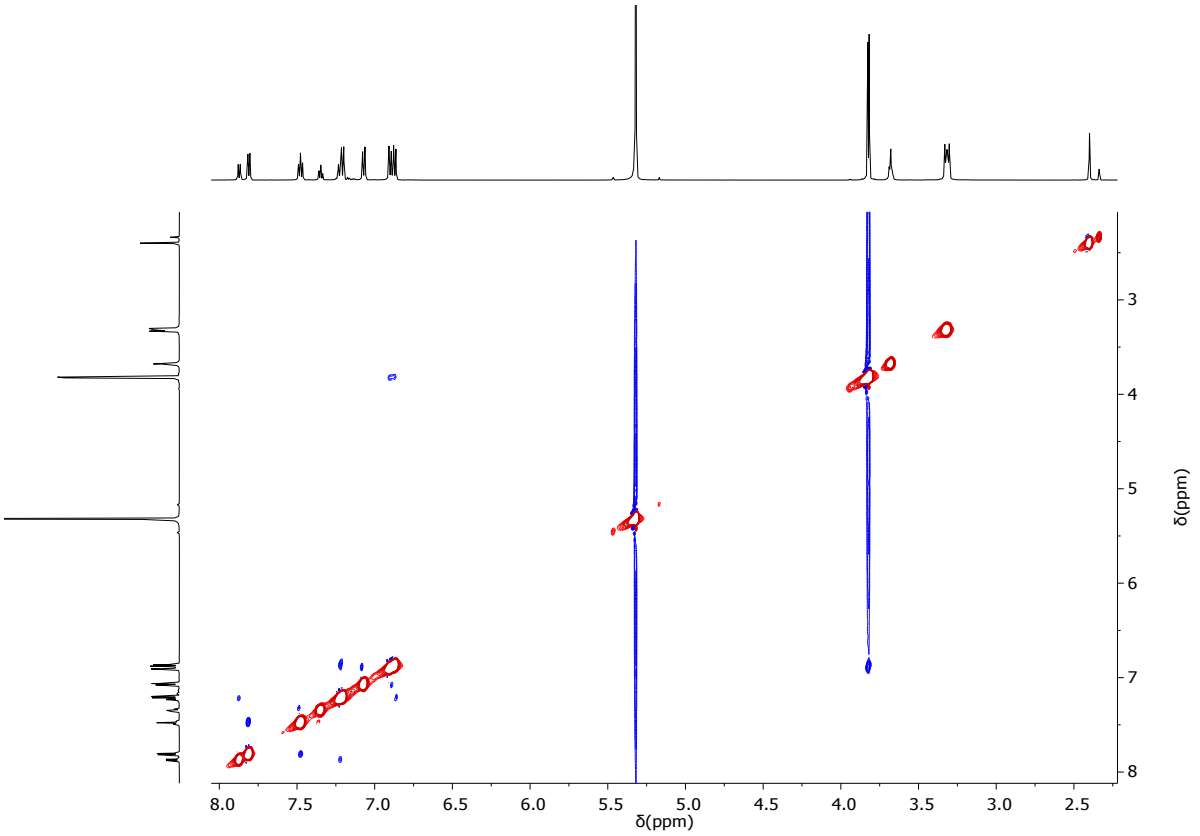

Figure S6c. ^{1}H-^{1}H NOESY spectrum of **5** + NBu_4Br (CD_2Cl_2, 600 MHZ, 25 °C).

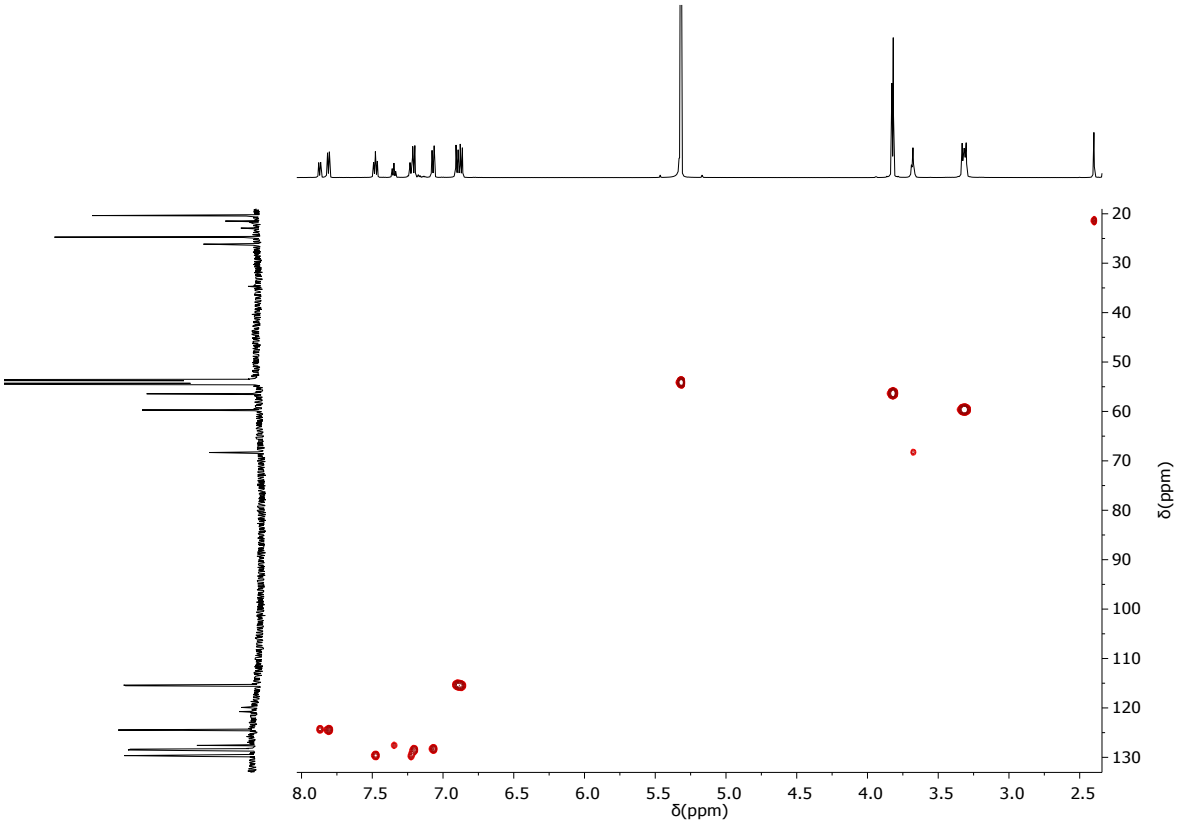

Figure S6d. ^{1}H-^{13}C gHSQC spectrum of **5** + NBu_4Br (CD_2Cl_2, 600 MHZ, 25 °C).

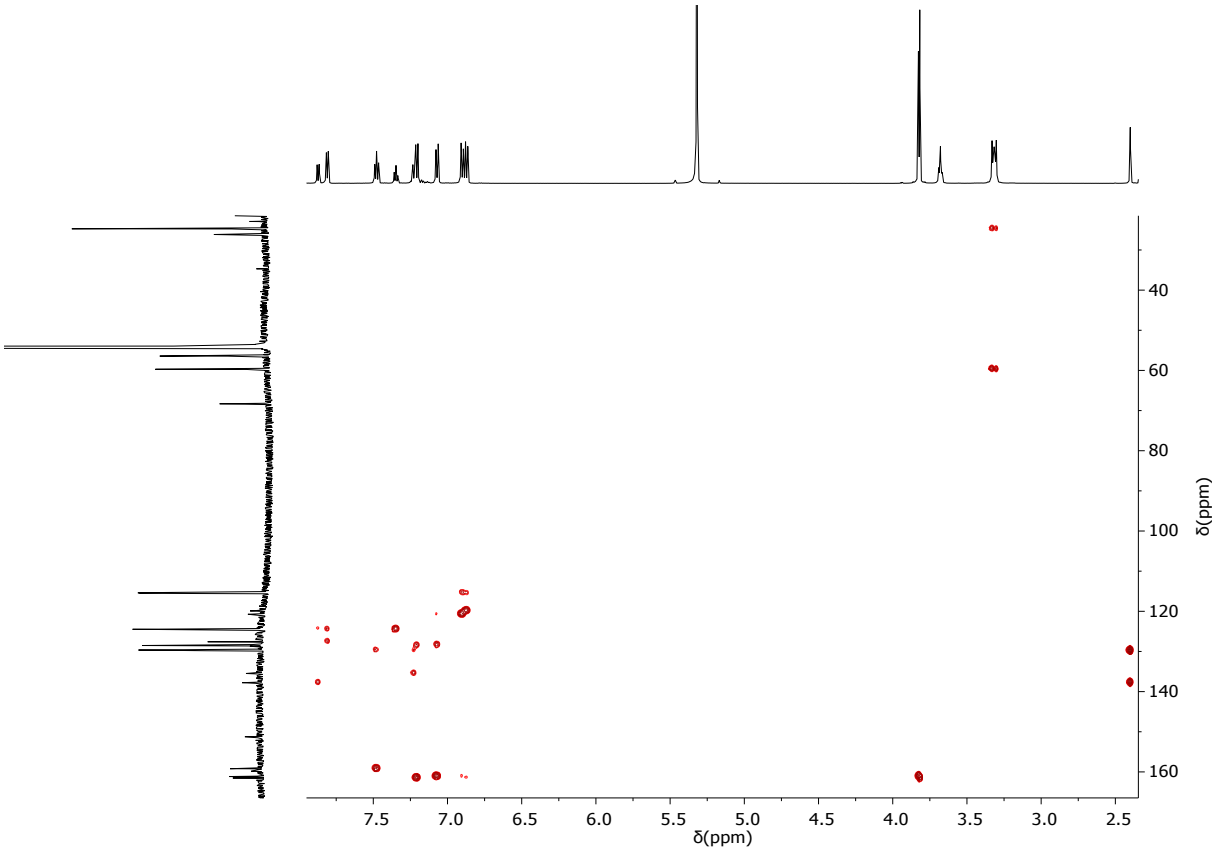

Figure S6e. ^{1}H-^{13}C gHMBC spectrum of **5** + NBu_4Br (CD_2Cl_2, 600 MHZ, 25 °C).

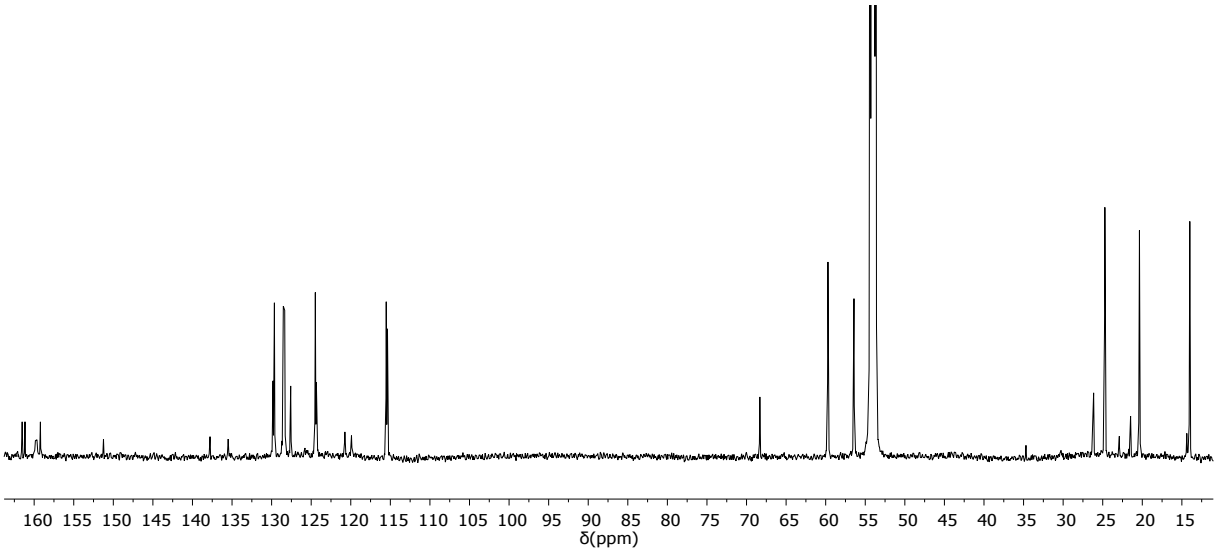

Figure S6f. ^{13}C NMR spectrum of **5** + NBu_4Br (CD_2Cl_2, 151 MHZ, 25 °C).

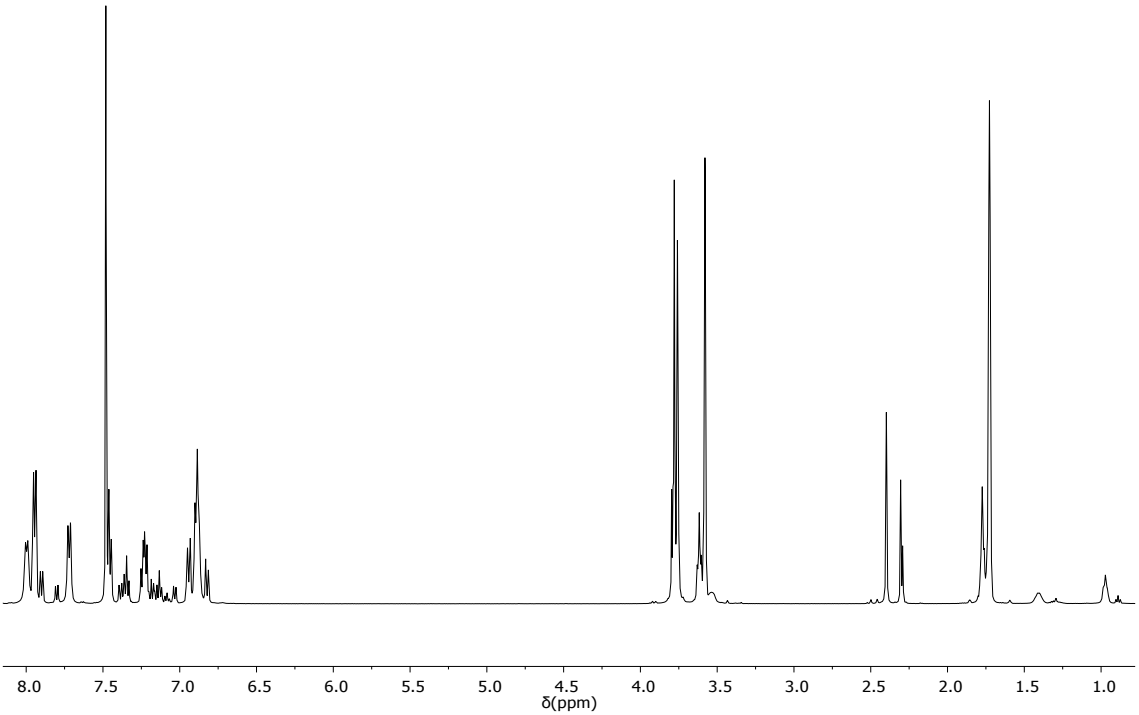

Figure S6g. ^{1}H NMR spectrum of **5** + NBu_4Br (THF-d_8, 500 MHZ, 25 °C).

In situ NMR reactivity studies

***In situ* NMR reaction of $FeBr_2(THF)_2$, Bu_4NBr and LK in THF-d_8**

In a glovebox a solution of **LK** (1 eq, 13.9 mg, $2.8 \cdot 10^{-2}$ mmol) in THF-d_8 was added dropwise to a vial containing $FeBr_2(THF)_2$ (1 eq, 10.0 mg, $2.8 \cdot 10^{-2}$ mmol) and Bu_4NBr (1 eq, 9.0 mg, $2.8 \cdot 10^{-2}$ mmol). The obtained red-purple mixture was transferred in a Young's NMR tube. The reaction was followed for 1 day at r.t. The ^1H NMR spectrum acquired after 1h shows **3** and **1** in ratio 1:1.2 (and 2% of LH) and after 1 day the ratio is 1:0.6. The reaction was warmed up to +60 °C for 4 days, during which the color turned fuchsia and **1** was converted almost completely to **3** (**3** and **1** in ratio 1:0.02).

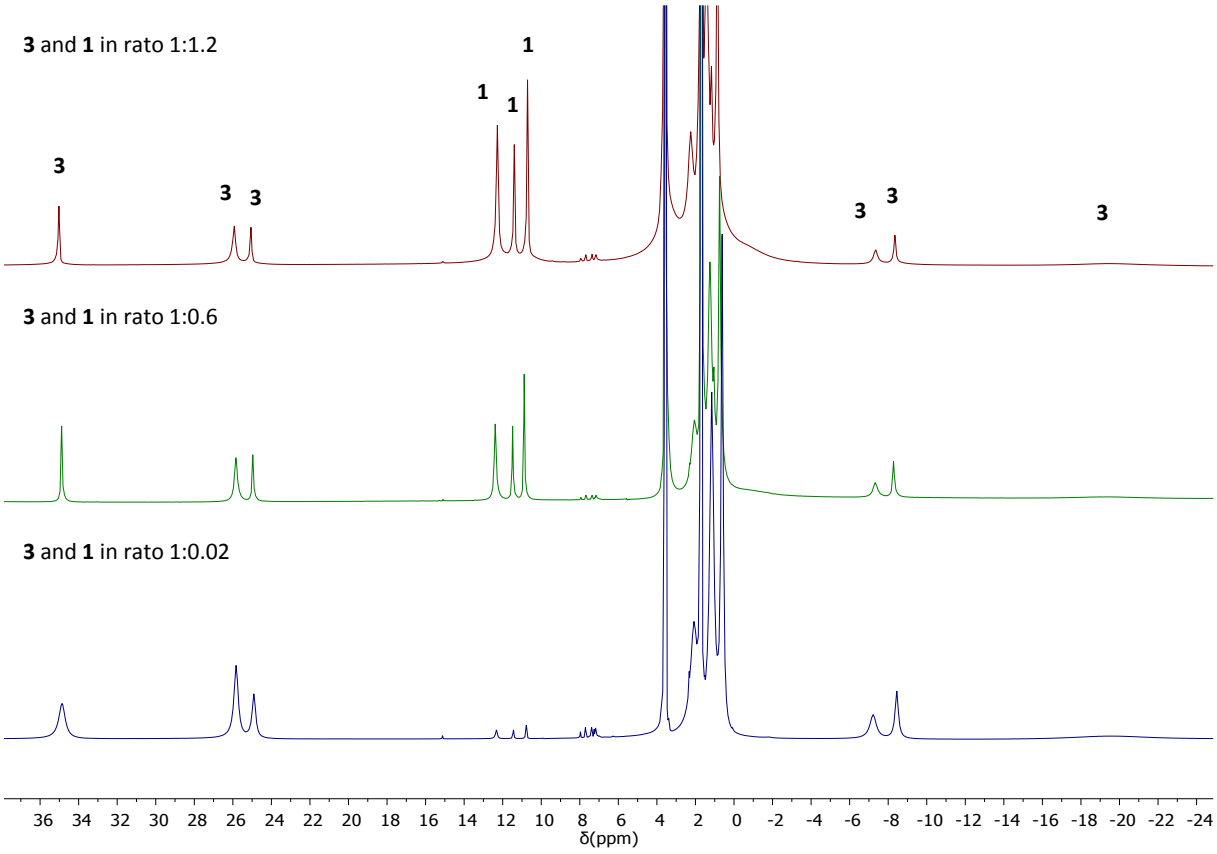

Figure S7. ^1H NMR spectrum of $FeBr_2(THF)_2$ (1 eq), Bu_4NBr (1 eq) and **LK** (1 eq) (THF-d_8, 400 MHZ, 25 °C): t = 1h at r.t. (red line), t = 1 day at r.t (green line), t = 1 day at r.t. + 4 days at +60 °C (blue line).

***In situ* NMR reaction of 1 + Bu_4NBr in toluene-d_8**

In a glovebox **1** (1 eq, 10.0 mg, $1.5 \cdot 10^{-2}$ mmol) and Bu_4NBr (2 eq, 9.7 mg, $1.5 \cdot 10^{-2}$ mmol) were mixed in toluene-d_8 in a Young's NMR tube.

The ^1H NMR spectrum acquired after 1h at r.t. shows **1** as major species. The reaction was warmed up to +60 °C for 1 day and then to +90 °C for 3 days, during which **1** was completely consumed and broad peaks for **3** and $[Bu_4N][L]$ appeared (the low intensity of the signals is due to the low solubility of these two compounds in toluene-d_8).

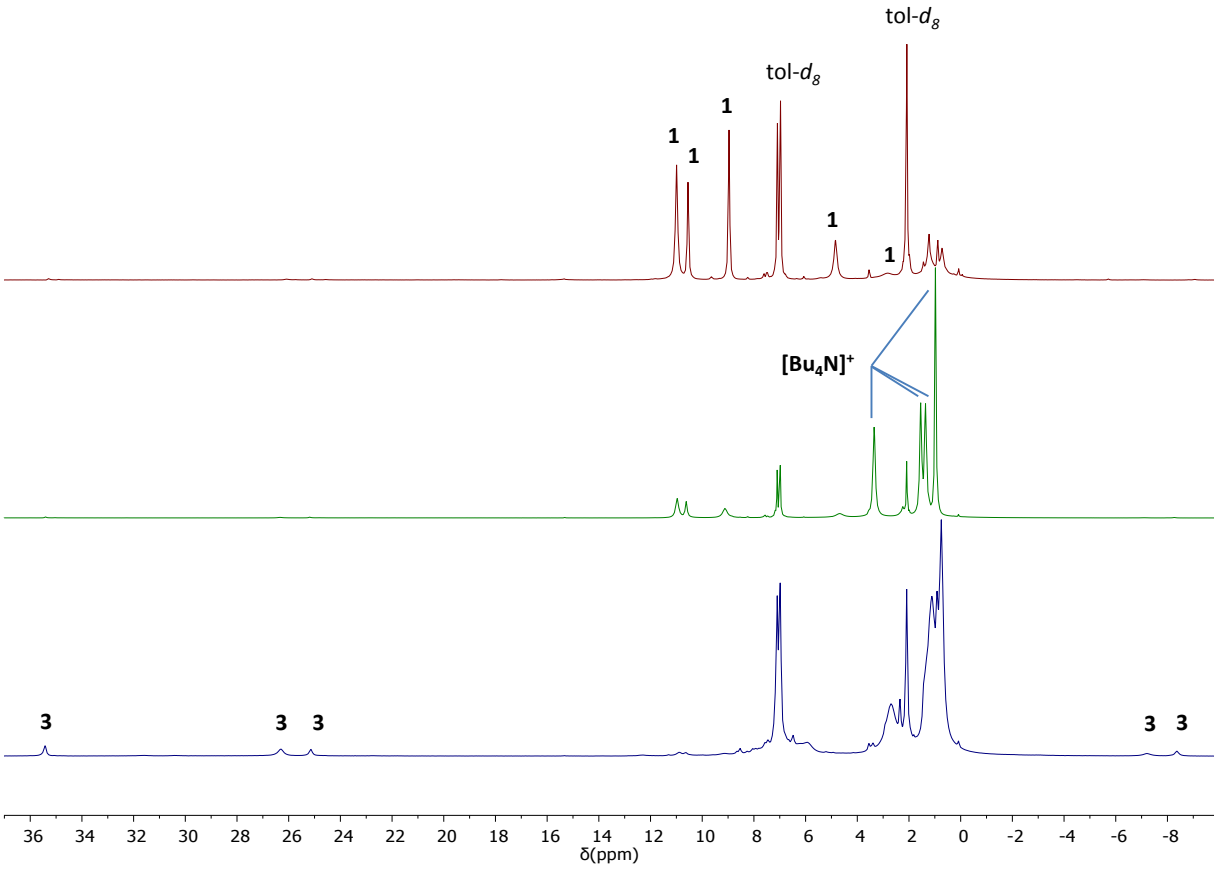

Figure S8. ^1H NMR spectrum **1** (1 eq) and Bu_4NBr (2 eq) (toluene-d_8, 400 MHZ, 25 °C): t = 1h at r.t. (red line), t = 1 day at +60 °C (green line), t = 1 day at +60 °C + 3 days at +90 °C (blue line).

Cyclic voltammetry

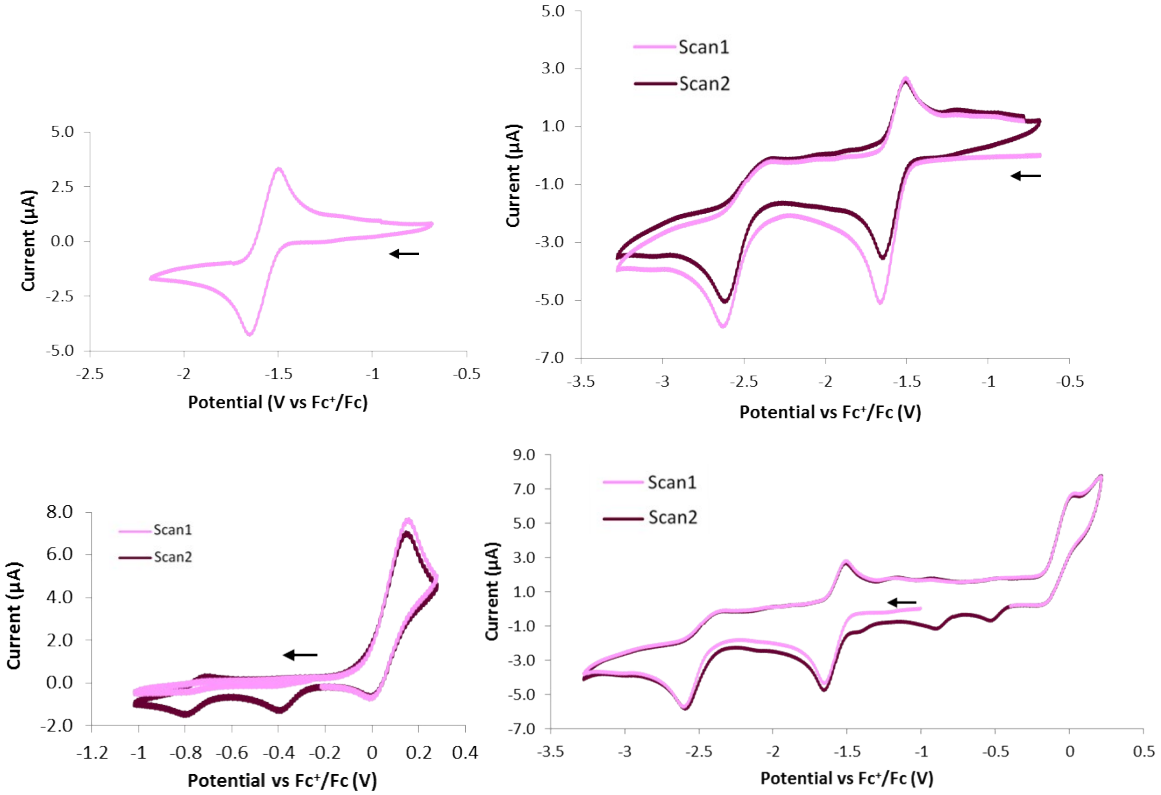

Figure S9. Cyclic voltammograms of compound **3** (ca. 1.50 mM solution of complex in THF; 0.1 M $[Bu_4N][PF_6]$ electrolyte; scan rate = 0.1 $V \cdot s^{-1}$).

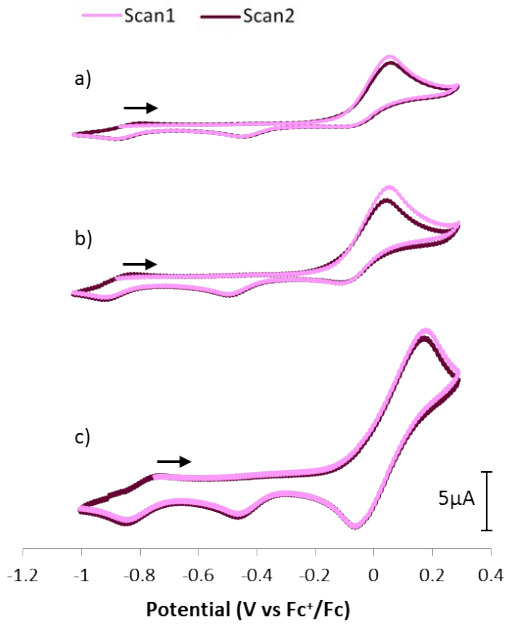

Figure S10. Cyclic voltammogram of compound **3** (ca. 1.50 mM solution of complex in THF; 0.1 M $[Bu_4N][PF_6]$ electrolyte, scan rate: a) 0.05 $V \cdot s^{-1}$, b) 0.1 $V \cdot s^{-1}$, c) 0.5 $V \cdot s^{-1}$).

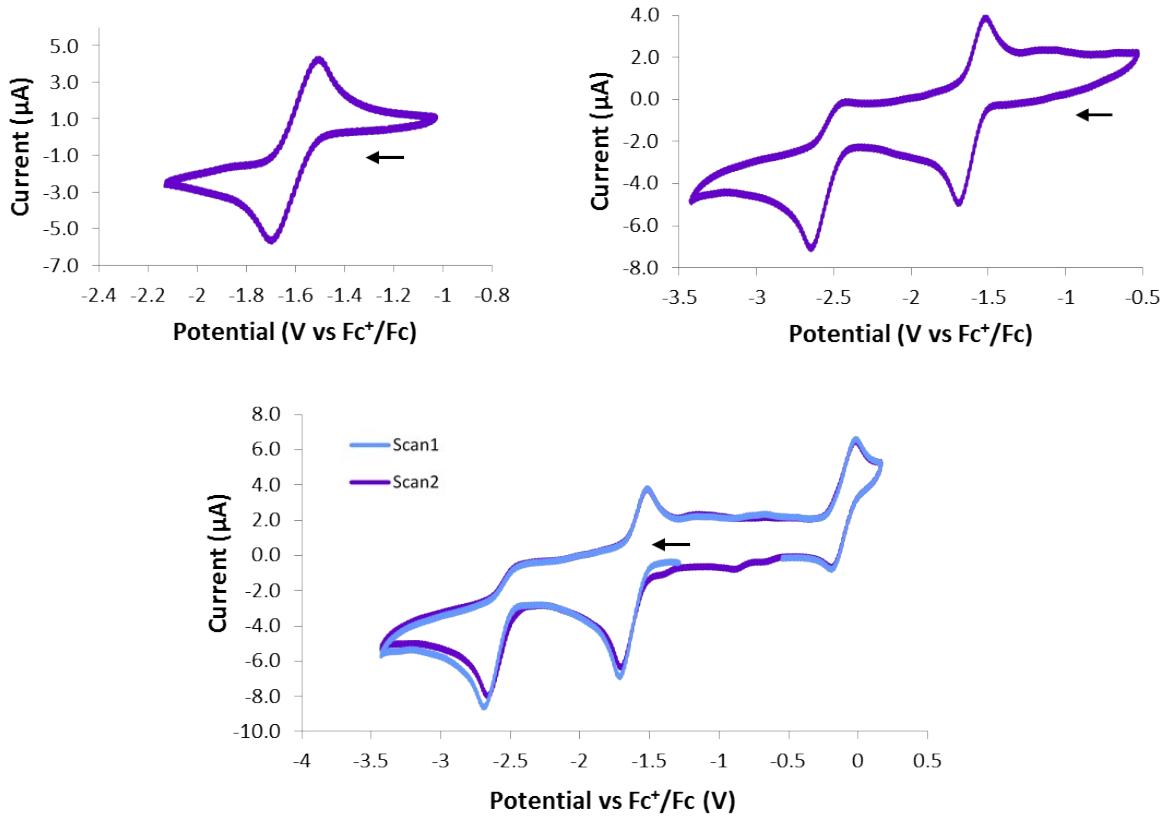

Figure S11. Cyclic voltammograms of compounds **4** (ca. 1.50 mM solution of complex in THF; 0.1 M $[Bu_4N][PF_6]$ electrolyte; scan rate = 0.1 $V \cdot s^{-1}$).

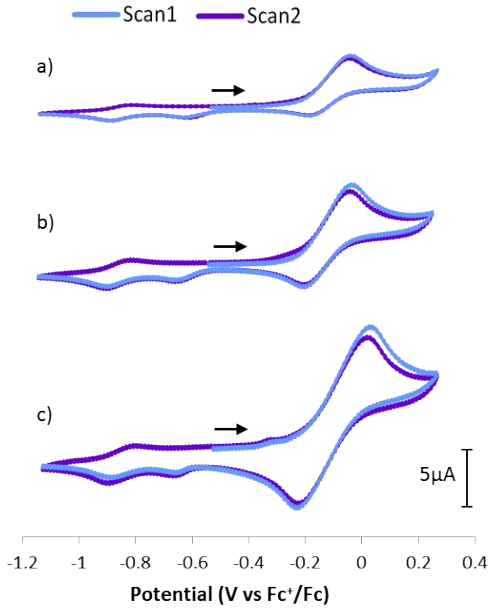

Figure S12. Cyclic voltammogram of compounds **4** (ca. 1.50 mM solution of complex in THF; 0.1 M $[Bu_4N][PF_6]$ electrolyte, scan rate: a) 0.05 $V \cdot s^{-1}$, b) 0.1 $V \cdot s^{-1}$, c) 0.3 $V \cdot s^{-1}$).

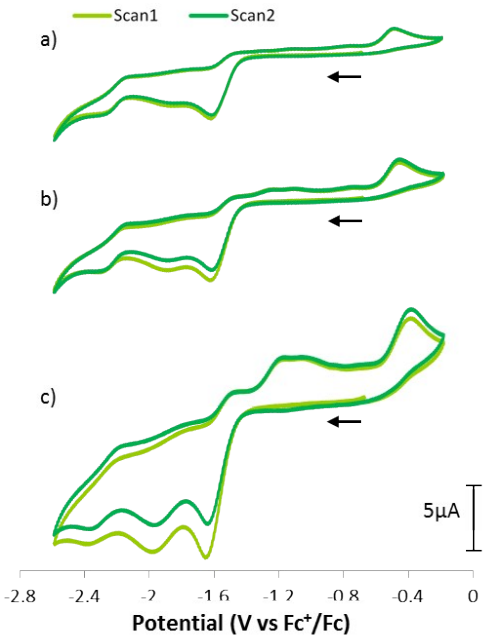

Figure S13. Cyclic voltammogram of compound **5** (ca. 1.50 mM solution of complex in 1,2-dichloroethane; 0.1 M $[Bu_4N][PF_6]$ electrolyte; scan rate: a) 0.05 $V \cdot s^{-1}$, b) 0.1 $V \cdot s^{-1}$, c) 0.5 $V \cdot s^{-1}$).

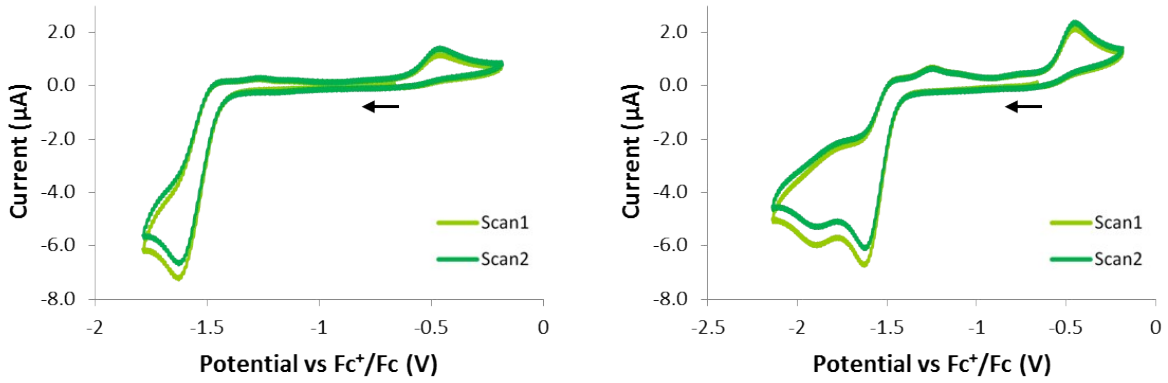

Figure S14. Cyclic voltammograms of compounds **5** (ca. 1.50 mM solution of complex in THF; 0.1 M $[Bu_4N][PF_6]$ electrolyte; scan rate = 0.1 $V \cdot s^{-1}$).

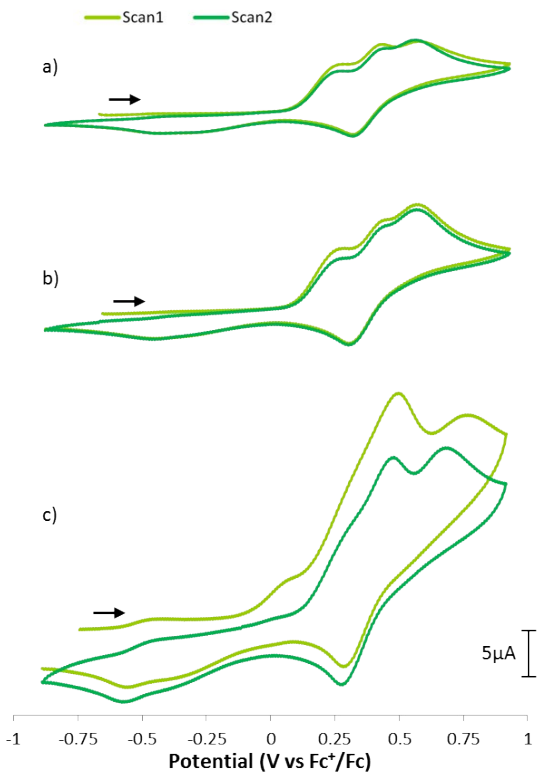

Figure S15. Cyclic voltammogram of compound **5** (ca. 1.50 mM solution of complex in 1,2-dichloroethane; 0.1 M $[Bu_4N][PF_6]$ electrolyte; scan rate: a) 0.05 $V \cdot s^{-1}$, b) 0.1 $V \cdot s^{-1}$, c) 0.5 $V \cdot s^{-1}$).

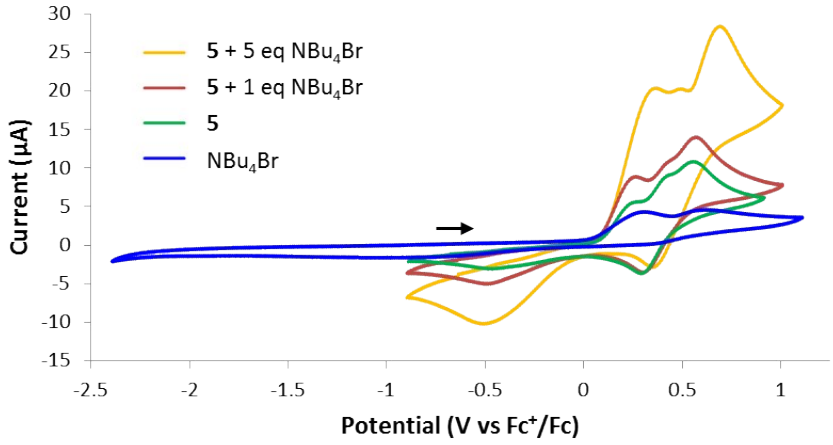

Figure S16. Cyclic voltammogram of compound **5**[1] with additional NBu_4Br (ca. 1.50 mM solution of complex in 1,2-dichloroethane; 0.1 M $[Bu_4N][PF_6]$ electrolyte; scan rate 0.1 $V \cdot s^{-1}$).

[1] Compound **5** was isolated as a mixture with Bu_4NBr: the voltammograms with added Bu_4NBr refer to equivalents in addition to that already present in **5**

UV-Vis absorption spectroscopy

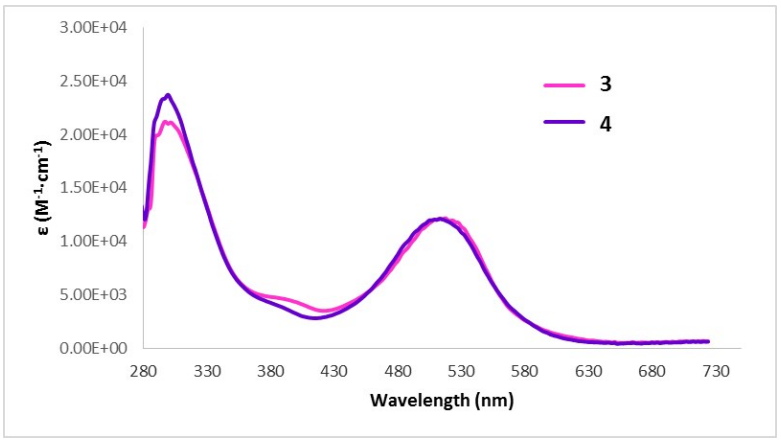

Figure S17. UV-Vis absorption spectra of compound **3** (pink line) and **4** (violet line) in THF.

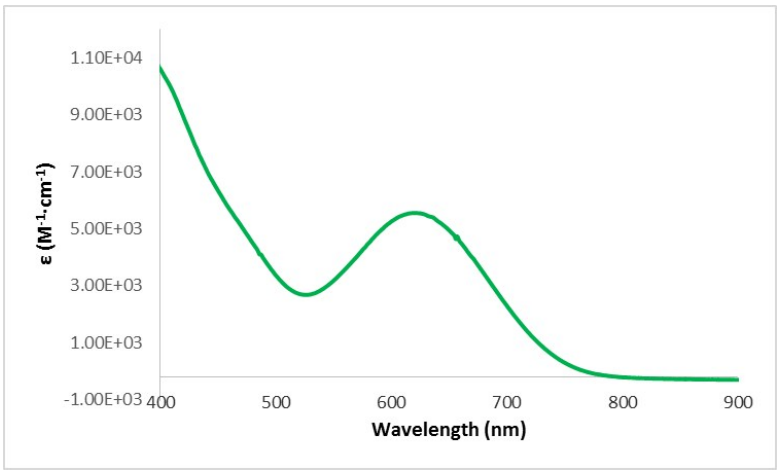

Figure S18. UV-Vis absorption spectrum of compound **5** in CH_2Cl_2.

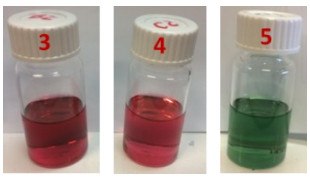

Figure S19. Physical appearance of compound **3** and **4** in THF and **5** in CH_2Cl_2.

Infrared spectroscopy

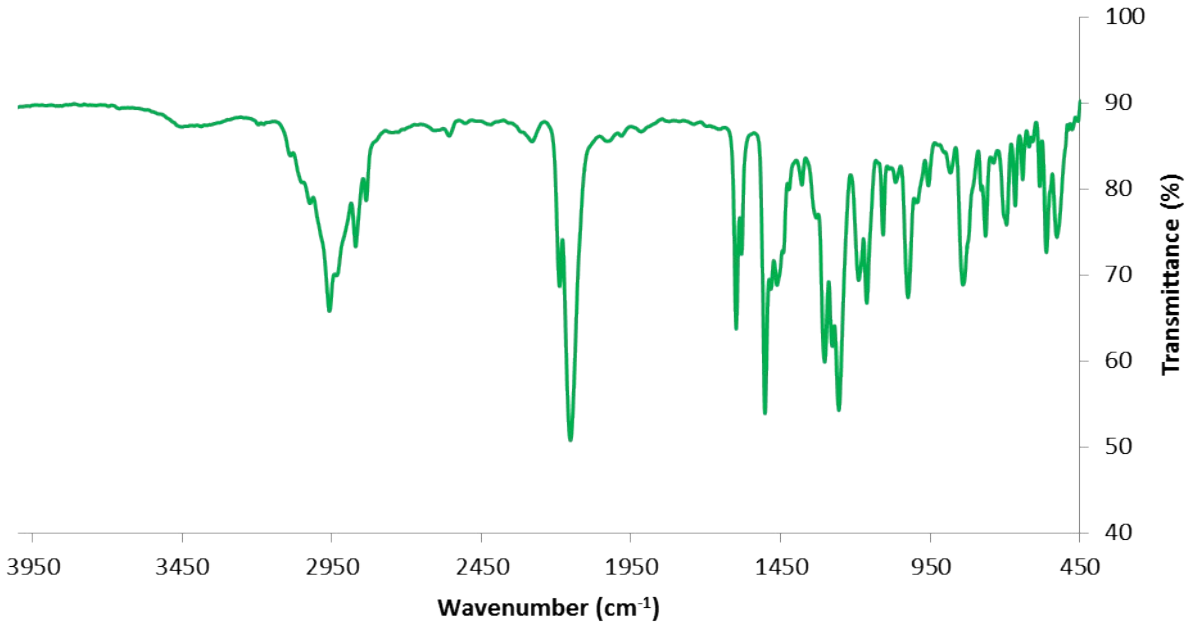

Figure S20. IR spectrum of compound **5** in the solid state.

References

(1) Bruker. *APEX3, SAINT and SADABS. Bruker AXS Inc., Madison, Wisconsin, USA*. **2016**.
(2) Sheldrick, G. *Acta Cryst. A* **2008**, *64*, 112.
(3) Sheldrick, G. *Acta Cryst. C* **2015**, *71*, 3.